14th International Conference on Applications of Statistics and Probability in Civil Engineering, ICASP14
Dublin, Ireland, July 9-13, 2023

Copula-based Quadratic Point Estimate Method for Probabilistic Moments Evaluation

Minhyeok Ko
PhD Candidate, Dept. of Civil & Environmental Engineering, The Pennsylvania State University, University Park, PA, USA

Konstantinos G. Papakonstantinou
Associate Professor, Dept. of Civil & Environmental Engineering, The Pennsylvania State University, University Park, PA, USA

ABSTRACT: As an extension to the Point Estimate Method (PEM) to evaluate probabilistic moments of quantities of interest (QoI) in general *n*-dimensional spaces, the Quadratic Point Estimate Method (QPEM) has been recently developed. This new method is defined to fully represent up to fifth-order input moments in the Gaussian space, providing general analytical expressions for sample locations and weights, without any optimization procedure requirements. The QPEM can significantly improve the estimation accuracy of the output QoI moments, in relation to PEM-based methods with linear samples increase with respect to the involved problem dimensions, while at the same time having an affordable and competitive computational cost up to a considerable number of dimensions. The QPEM is further enhanced and generalized in this work by enabling copula integration into the framework, which enables effective modeling of the joint input probability density function by estimating marginals and the dependence structure of the involved random variables. The validity and outstanding performance of the copula-based QPEM are showcased against numerous other sampling methods in various examples with emphasis on geotechnical applications where PEM-based methods have a long history of development and successful implementations.

1. INTRODUCTION

In many engineering applications, Uncertainty Quantification (UQ) through a nonlinear model often entails calculating probabilistic moment integrals. For calculating these numerical integrations, the Monte Carlo method (MC) is the most versatile and widely used sampling technique employed in engineering. The MC method generally requires a considerable number of samples that may be very computationally expensive if an engineering problem involves computationally intensive simulations. Variance reduction techniques, such as quasi-Monte Carlo methods (QMC) and Latin Hypercube Sampling (LHS), can be alternatives to the MC method and can offer the advantage of faster convergence up to certain dimensions, in relation to the number of performed simulations. Quadrature techniques have also been utilized for the estimation of the moment integrals, and, overall, they work well in deterministic cases. In probabilistic problems, however, such techniques can be prohibitive when high-dimensional spaces are involved.

The development of relevant dedicated probabilistic methods, such as the Point Estimate Method (PEM) also has a long history. The concept of PEM was first introduced by Rosenblueth (1975). Since then, many PEM variations have been developed that are generally powerful yet simple approximation methods used to estimate the first few moments of an output Probability Density Function

(PDF). In many cases, PEM-based methods provide noticeably accurate mean and standard deviation estimations, with notable computational efficiency. However, most existing PEMs are unsuitable for higher-order moments estimation with low computational cost, such as skewness and kurtosis. This accuracy largely depends on their ability to accurately describe high-order input moments, with more sampling points (also called sigma points) generally required for this. Hence, the main computational cost of the PEMs is relevant to the utilized number of sigma points, and there is a natural trade-off between computational efficiency and estimation accuracy concerning this number. In addition, PEMs often use an optimization procedure to find the sigma points locations and weights (Rosenblueth, 1975) which might be an undesirable practice in many problems.

Motivated by the aforementioned, a Quadratic Point Estimate Method (QPEM) has been recently proposed, to improve the moment estimation accuracy taking also the computational cost into consideration (Ko and Papakonstantinou, 2023). The QPEM completely captures up to fifth-order input moments of the Gaussian distributions, without requiring any expensive optimization procedures to determine the sigma point characteristics. In addition, it can control/reduce some errors of output moment estimation without additional sampling points, in contrast to other PEMs.

A suitable joint PDF input model $f(\mathbf{x})$ is needed in probabilistic analysis, and quite often Gaussian distributions are employed. This Gaussian assumption introduces a convenient representation of input dependencies. However, the real dependence structure may not adhere to this assumption.

Recently, dependence modeling has seen significant advances with the widespread adoption of copula models, including vine copulas. In higher dimensions, constructing multivariate dependencies that suitably define the couplings and interactions is a challenging problem. Vine copulas, first established by Joe (1997), ease this construction by expressing the multivariate dependence as a product of bivariate copulas among pairs of random variables. As a result, the vine models provide an easy interpretation and are extremely flexible in constructing the joint PDF.

In this work, the QPEM is further enhanced and generalized by enabling vine copulas integration into the framework, which enables effective modeling of the joint input PDF by estimating marginals and representing dependencies of the random variables based on available data. The validity and outstanding performance of copula-based QPEM are showcased against numerous other sampling methods based on two geotechnical applications, where PEM related methods have a long history of development and successful implementations.

2. QUADRATIC POINT ESTIMATE METHOD

Recently, Ko and Papakonstantinou (2023) developed the QPEM to overcome drawbacks of existing PEMs with respect to accuracy, efficiency, and practicality. The QPEM has three main properties, as follows: (a) fully symmetric sigma points that can satisfy odd-order moments of zero automatically; (b) general, analytical expressions for sigma points and associate weights, avoiding the likely undesirable optimization process; and (c) ability to often offer reduced errors in higher-order output moments without additional computational cost.

The QPEM can completely capture up to fifth-order moments of the n-$\mathbb{D}$ standard Gaussian random variable $\mathbf{z}$. Figure 1 shows the fully symmetric sigma points of the QPEM and the corresponding point types based on their weights. Three types of points are used: (a) 1st type is a single point that lies at the origin point $\mathbf{0}$ with weight w_0; (b) 2nd type

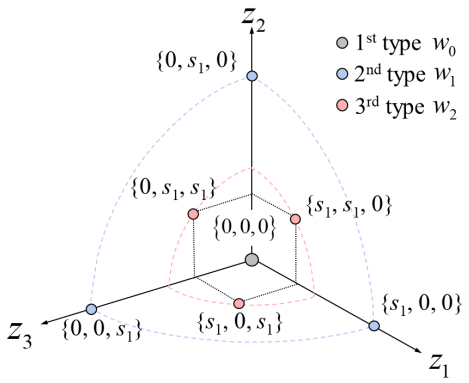

Figure 1: Sigma points of QPEM in 3-$\mathbb{D}$

Table 1: Sigma points and weights selection for QPEM

Weights		$W_0^{(1)} = W_0^{(2)} = w_0 \quad W_0^{(3)} = w_0 + \zeta \quad W_0^{(4)} = w_0 + \xi$ $W_i^{(k)\,a} = \begin{cases} w_1, & \text{for } i = 1, \cdots, 2n \\ w_2, & \text{for } i = 2n+1, \cdots, 2n^2 \end{cases}$
Sigma Point	1st type	$\mathbf{S}_0 = \mathbf{0}_{n\times 1}$
	2nd type	$\mathbf{S}_1 = \{s_1, 0, \cdots, 0\}^T \quad \cdots \quad \mathbf{S}_n = \{0, \cdots, 0, s_1\}^T$ $\mathbf{S}_{n+1} = \{-s_1, 0, \cdots, 0\}^T \quad \cdots \quad \mathbf{S}_{2n} = \{0, \cdots, 0, -s_1\}^T$
	3rd type	$\mathbf{S}_{2n+1} = \{s_2, s_2, 0, \cdots, 0\}^T \quad \cdots \quad \mathbf{S}_{2n^2-3} = \{0, \cdots, 0, s_2, s_2\}^T$ $\mathbf{S}_{2n+2} = \{-s_2, s_2, 0, \cdots, 0\}^T \quad \cdots \quad \mathbf{S}_{2n^2-2} = \{0, \cdots, 0, -s_2, s_2\}^T$ $\mathbf{S}_{2n+3} = \{s_2, -s_2, 0, \cdots, 0\}^T \quad \cdots \quad \mathbf{S}_{2n^2-1} = \{0, \cdots, 0, s_2, -s_2\}^T$ $\mathbf{S}_{2n+4} = \{-s_2, -s_2, 0, \cdots, 0\}^T \quad \cdots \quad \mathbf{S}_{2n^2} = \{0, \cdots, 0, -s_2, -s_2\}^T$

[a] Associated weights for calculating k^{th} moments of the response function

consists of $2n$ points on the orthogonal axis with a distance s_1 from the origin point and has weight w_1; and (c) 3rd type includes $2n(n-1)$ points obtained by permutations and by changes of sign of the coordinates $\{s_2, s_2, 0, \cdots, 0\}^T$. The associated weight of the third type of points is w_2. In total, $2n^2$+1 points are required for the QPEM. The analytical solution of sigma points and weights is given as:

$$\begin{cases} s_0 = 0 \\ s_1 = r \\ s_2 = \left[\dfrac{r^2(n-1)}{r^2+n-4}\right]^{1/2} \end{cases} \quad \begin{cases} w_0 = 1 - 2nw_1 - 2n(n-1)w_2 \\ w_1 = \dfrac{4-n}{2r^4} \\ w_2 = \dfrac{1}{4}\left[\dfrac{r^2+n-4}{r^2(n-1)}\right]^2 \end{cases} \tag{1}$$

where r is an arbitrary user-defined tuning parameter, satisfying $r > \sqrt{2}$ due to QPEM stability. Depending on this parameter r, the error induced from moments higher than the fifth-order could be reduced. In this work, the default value of r is used as r=3, as suggested by Ko and Papakonstantinou (2023).

The sigma points can also include here partial higher-order input moments information than fifth-order by adopting the scaling parameters ζ and ξ, with no additional computational effort. These parameters are considered additional weights for the origin point $\mathbf{0}$ when estimating the third- and fourth-order moments, i.e., skewness or kurtosis. The sigma points and associated weights for the QPEM are provided in Table 1. For any input distribution, whether Gaussian or non-Gaussian, the sigma points, $\mathbf{S}_i$, are initially selected in the standard normal z-space, and are then translated to the original x-space using an appropriate transformation $\mathbf{X}_i$=$\mathscr{T}(\mathbf{S}_i)$. These transformed points are then propagated through the computational model $\mathbf{Y}_i = \mathbf{M}(\mathbf{X}_i)$. The first four moments of the response model are obtained as:

$$E[\mathbf{y}] \equiv \bar{\mathbf{y}} = \sum_{i=0}^{2n^2} W_i^{(1)} \mathbf{Y}_i \tag{2}$$

$$E\left[(\mathbf{y}-\bar{\mathbf{y}})^k\right] = \sum_{i=0}^{2n^2} W_i^{(k)} (\mathbf{Y}_i - \bar{\mathbf{y}})^k \tag{3}$$

Eq. (3) represents the kth-order moments estimation where k=2, 3, and 4. The kth-order moments are vectorized and expressed with the Kronecker product, $\otimes$, e.g., $E[(\mathbf{y}-\bar{\mathbf{y}})(\mathbf{y}-\bar{\mathbf{y}})^T] \equiv E[(\mathbf{y}-\bar{\mathbf{y}}) \otimes (\mathbf{y}-\bar{\mathbf{y}})] = E[(\mathbf{y}-\bar{\mathbf{y}})^2]$.

3. VINE COPULAS

3.1. Copulas and Sklar's theorem

A copula can be described by a multivariate cumulative distribution function (CDF), $C_{\mathbf{x}}$, that combines univariate marginal probability distributions with a particular dependence structure. A multivariate joint distribution with specified marginal distributions can be thus constructed for an appropriate C_n based on Sklar's theorem (Nelsen, 2007):

$$F(\mathbf{x}) = C_{\mathbf{x}}(F_1(x_1), \cdots, F_n(x_n)) \tag{4}$$

where F is a joint CDF with univariate CDFs $F_1, \cdots, F_n$. Eq. (4) shows that any joint CDF can be expressed in terms of its marginals and a n-$\mathbb{D}$ copula. Sklar's theorem can also be re-stated using

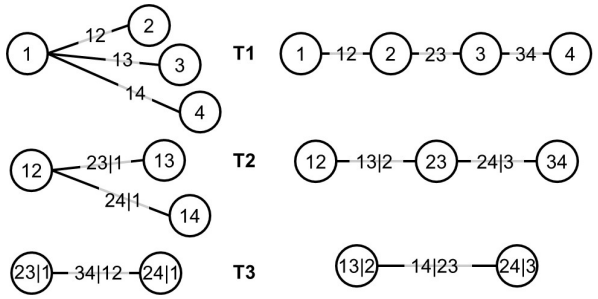

Figure 2: C-vine (left) and D-vine (right) in 4-$\mathbb{D}$

the chain rule as:

$$f(\mathbf{x}) = \frac{\partial^n F(\mathbf{x})}{\partial x_1 \dots \partial x_n} = c_{\mathbf{x}} \left\{ F_1(x_1), \dots, F_n(x_n) \right\} \cdot \prod_{i=1}^{n} f_i(x_i) \tag{5}$$

where $c_{\mathbf{x}}(\mathbf{u}) = \frac{\partial^n C_{\mathbf{x}}(\mathbf{u})}{\partial u_1 \dots \partial u_n}$ is a copula density function, and $f_i(x_i)$ are the marginal PDFs.

3.2. Vine copulas and Rosenblatt transforms

When the input dimension increases, defining a suitable $C_{\mathbf{x}}$ that properly describes the higher-order dependencies among the input variables becomes increasingly challenging. The main idea of vine copulas is hence to decompose a n-$\mathbb{D}$ copula density into bivariate copulas, also called pair-copulas, such that the n-$\mathbb{D}$ copula can be practically represented based on conditioning and a graphical tool, as shown in Figure 2. The structures are also known as *vines* and, depending on their formation, different pair-copula constructions emerge, as the C-vine and D-vine ones in Figure 2. For further details, we refer to (Bedford and Cooke, 2002; Aas et al., 2009).

The joint PDF $f(\mathbf{x})$ can be then factorised as:

$$f(\mathbf{x}) = f(x_1) f(x_2 \mid x_1) \cdots f(x_n \mid x_1, \cdots, x_{n-1}) \tag{6}$$

where the univariate conditional PDFs in the general form of $f(x_i \mid \mathbf{v})$ can be expressed as:

$$f(x_i \mid \mathbf{v}) = c_{x_i v_j \mid \mathbf{v}_{-j}} \left\{ F\left(x_i \mid \mathbf{v}_{-j}\right), F\left(v_j \mid \mathbf{v}_{-j}\right) \right\} \cdot f\left(x_i \mid \mathbf{v}_{-j}\right) \tag{7}$$

where v_j is an arbitrarily excluded element from vector $\mathbf{v}$, and $\mathbf{v}_{-j}$ denotes the vector excluding v_j. By combining Eqs. (6) and (7), we can derive a decomposition of $f(\mathbf{x})$ that only consists of marginal distributions and pair-copulas. The joint PDF $f(\mathbf{x})$ corresponding to the C-vine in Figure 2, for instance, is expressed as:

$$\begin{aligned} f(\mathbf{x}) = {} & f_1(x_1) \cdot f_2(x_2) \cdot f_3(x_3) \cdot f_4(x_4) \\ & \cdot c_{x_1 x_2} \left\{ F(x_1), F(x_2) \right\} \cdot c_{x_1 x_3} \left\{ F(x_1), F(x_3) \right\} \\ & \cdot c_{x_1 x_4} \left\{ F(x_1), F(x_4) \right\} \cdot c_{x_2 x_3 \mid x_1} \left\{ F(x_2 \mid x_1), F(x_3 \mid x_1) \right\} \\ & \cdot c_{x_2 x_4 \mid x_1} \left\{ F(x_2 \mid x_1), F(x_4 \mid x_1) \right\} \\ & \cdot c_{x_3 x_4 \mid x_1 x_2} \left\{ F(x_3 \mid x_1, x_2), F(x_4 \mid x_1, x_2) \right\} \end{aligned} \tag{8}$$

We should note that there are various forms to decompose $f(\mathbf{x})$ because of many different choices of v_j, as also illustratively shown in Figure 2. The C-vine and D-vine are two major types of regular vines. The vine copulas involve marginal conditional distributions of the form $F(x_i \mid \mathbf{v})$ which can be evaluated using a recursive formula derived as (Joe, 1997):

$$F(x_i \mid \mathbf{v}) = \frac{\partial C_{x_i v_j \mid \mathbf{v}_{-j}} \left\{ F\left(x_i \mid \mathbf{v}_{-j}\right), F\left(v_j \mid \mathbf{v}_{-j}\right) \right\}}{\partial F\left(v_j \mid \mathbf{v}_{-j}\right)} \tag{9}$$

A general transformation that maps an input vector $\mathbf{X}$ onto a vector $\mathbf{Z}$ with independent components is the Rosenblatt transform. Its inverse transforms reversely the independent random variables into dependent ones. However, the Rosenblatt transformation and its inverse require knowledge of a joint PDF, or several conditional ones, which are hardly known in practical applications. The vine copulas can thus alleviate this issue by enabling one to construct such a joint PDF even for complex high-dimensional cases.

4. COPULA-BASED QPEM

The Rosenblatt transformation supported by the vine copulas could allow the QPEM to be more flexible in modeling the complex dependencies between variables. However, there are many different ways of representing a joint PDF with vine copulas. The critical step for the PDF construction thus lies in the determination of the vine structure and its parameters based on available information. Given, in particular, a vine model of the input dependencies, inferred from available data, the z-space generated sigma points can be mapped onto the original x-space by the inverse Rosenblatt transformation.

Table 2: Algorithm of copula-based QPEM for cases with arbitrary distributions and complex dependence structures

Input: Available data $(x_{\ell 1}, \ldots x_{\ell n}), \ell = 1, \ldots, N$.
Output: First four output moments.
1: Determine regular vine copula specification.
1.1: Select T_1 that maximizes the sum of the absolute empirical Kendall's τ using Maximal Spanning Tree (MST) (Cormen et al., 2022).
1.2: Fit and select the pair-copula families (copula and corresponding parameters) in T_1 based on the Stepwise Semiparametric Estimator (SSP) with the lowest AIC (Haff, 2013).
1.3: Apply again MST to the graph of all nodes of T_2 with all edges allowed by proximity.
1.4: Continue alike with the remaining trees.
2: Fit and select marginals based on the given data.
3: Construct the joint PDF based on the selected vine copulas and marginals.
4: Generate sigma points and weights in z-space with Eq. (1).
5: Transform sigma points generated in z-space into the original x-space using an inverse Rosenblatt transformation supported by the computed vine copulas and marginals.
6: Estimate probabilistic output moments with Eqs. (2) and (3).

As mentioned, however, since the number of possible vine structures grows rapidly with the dimensions, it is generally infeasible to find the globally best-fitted vine copula. Dißmann et al. (2013) developed a sequential heuristic method to select a regular vine structure. Starting by defining the first tree T_1 of the vine based on available data, the rest of the vine structure is sequentially determined, $T_2, \ldots, T_{n-1}$. Even though this process still does not guarantee a global optimum, because every tree is examined separately, the determined vine structure is a reasonable one (Dißmann et al., 2013). The general algorithm of the copula-based QPEM is summarized in Table 2. For the details of MST and SSP in the sequential method, we refer to the cited literature. Kendall rank correlation coefficient, commonly referred to as Kendall's τ, is used in this work as a measure of dependence, since it can measure dependence independently of the distribution type.

5. NUMERICAL EXAMPLES

In this section, the following two examples are studied to evaluate the copula-based QPEM. MC simulation with 10^6 samples is used as a reference solution in this work. In order to compare with the copula-based QPEM with $2n^2+1$ needed samples, variance reduction sampling techniques, i.e., LHS and QMC with $2n^2+1$ samples, sparse grid quadrature, i.e., Smolyak Gauss-Hermite quadrature (SGH3) with $2n^2+2n+1$ needed samples, and one of the most well-known and popular PEMs, Hong's PEM (HPEM) (Hong, 1998), with $2n+1$ needed samples have been employed.

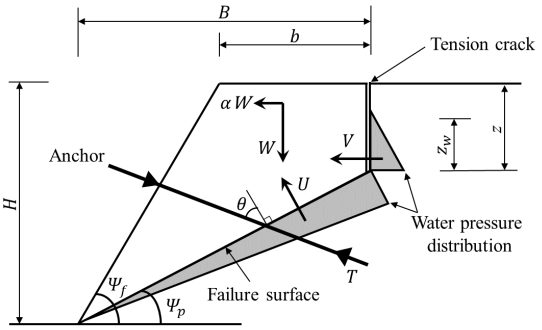

Figure 3: Schematic representation of a rock slope

5.1. Rock slope example

This example considers a two-dimensional rock slope with a water-filled tension crack, shown in Figure 3. The factor of safety for the slope is given as (Hoek, 2007):

$$F_s(\mathbf{X}) = \frac{hA + N' \tan\phi}{W(\sin\psi_p + \alpha\cos\psi_p) + V\cos\psi_p - T\sin\theta} \tag{10}$$

Table 3: Marginals of random variables of the rock slope example

Variable	Distribution	Mean	STD[a]
h $[kPa]$	Lognormal	140	14
ϕ $[^\circ]$	Lognormal	30	3
z $[m^2]$	Lognormal	14	2.1
r	Truncated Exponential [0,1]	0.3	0.3
α $[g]$	Truncated Exponential [0,0.15]	0.02	0.02

[a]STD=standard deviation

where

$$
\begin{aligned}
A &= (H-z)/\sin\psi_p \\
z &= H\left(1-\sqrt{\cot\psi_f \tan\psi_p}\right) \\
N' &= W(\cos\psi_p - \alpha\sin\psi_p) - U \\
&\quad -V\sin\psi_p + T\cos\theta \\
W &= 0.5\gamma H^2\{[1-(z/H)^2]\cot\psi_p - \cot\psi_f\} \\
U &= 0.5\gamma_w z_w A \\
V &= 0.5\gamma_w z_w^2 \\
r &= z_w/z
\end{aligned}
$$

in which γ=unit weight of rock=$2.6\times10^4 N/m^3$, γ_w=unit weight of water=$1.0\times10^4 N/m^3$, ψ_f=angle of slope=50°, ψ_p=angle of failure surface=35°, T=force applied by anchor system=0N, θ=inclination of anchor=0° and H=height of the overall slope=60m. Five random variables (n=5) are involved in this case: the cohesion h and the friction angle ϕ of the failure surface; the tension crack depth z; the height of water z_w in the tension crack; and the horizontal earthquake acceleration α. The information regarding their marginals is tabulated in Table 3.

We assume here that $h-\phi$ and $r-z$ are correlated respectively with Frank copula rotated by 90° (θ=2) and t-copula (ρ=-0.6, ν=10). There are no other variable dependencies assumed in this example. 500 random samples have been generated and are considered as the available data. Based on these data, the vine copula specification is estimated by the sequential method explained in Section 4. Having now defined the input model, the first four moments of the response model in Eq. (10) can be estimated. The computed results based on all used methods are summarized in Table 4. The relative error of each method is plotted in Figure 4.

Generally, the first two moments are estimated reasonably compared to the higher-order moments.

Table 4: Moment estimations for the rock slope example

Method	Sample size	Mean	STD	Skewness	Kurtosis
MC	10^6	1.5409	0.1223	0.1281	3.1326
LHS	51	1.5429	0.1357	0.8177	4.0762
QMC	51	1.5389	0.1025	0.3359	2.5612
SGH3	61	1.5404	0.1250	0.1123	2.6267
HPEM	11	1.5417	0.1347	0.4462	2.1086
QPEM	51	1.5406	0.1257	0.1197	2.9809

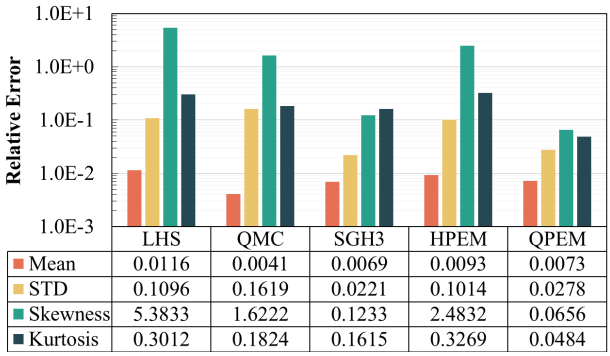

Figure 4: Relative errors related to the rock slope example

For the skewness and kurtosis, however, LHS and QMC have a substantial relative error, because their 51 sample points, as many as the QPEM ones ($2\times5^2+1$), are not sufficient to achieve accurate results. In contrast, the QPEM has a much lower relative error for the skewness (6.56%) and kurtosis (4.84%) than these variance reduction sampling methods. The SGH3 seems quite competitive in calculating the first two output moments, but the quadrature technique indicates quite higher errors for the higher-order output moments. The reason is that the SGH3 produces significant errors in representing the higher-order input moments compared to the QPEM. In this example, it can be seen that the copula-based QPEM offers a quite accurate approximation of the first four moments of the highly nonlinear response function and it is overall more efficient than the other utilized methods.

5.2. *Rock tunnel excavation example*

This example involves a rock tunnel excavation adapted from (Li and Low, 2010). The tunnel excavation problem is shown in Figure 5, and significant stresses and displacements can be present in the rock mass near the excavation site. The analytical solution for the induced inward displace-

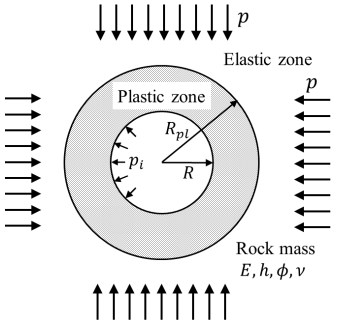

Figure 5: Schematic drawing of a circular tunnel excavation in a rock mass

ment based on the Mohr-Coulomb failure criterion is given as:

$$u_{ip} = R\left[(1+\nu)/E\right]\left[2(1-\nu)\left(p-p_{cr}\right)\left(R_{pl}/R\right)^2 - (1-2\nu)\left(p-p_i\right)\right] \tag{11}$$

where R=radius of excavation of a circular tunnel, u_{ip}=the inward displacement of the tunnel lining, p=the hydrostatic pressure, E=the Young's modulus, ν=the Poisson's ratio, and p_{cr}=critical pressure=$\frac{2p-\sigma_c}{k+1}$ in which k=$\frac{1+\sin\phi}{1-\sin\phi}$, σ_c=$\frac{h(k-1)}{\tan\phi}$, h=cohesion, and ϕ=friction angle. The uniform support pressure p_i is considered here deterministic with a value of $0.868MPa$. If p_i is less than p_{cr}, a plastic zone exists, and the radius of the plastic zone R_{pl} is given as:

$$R_{pl} = R\left[\frac{2(p+s)}{(k+1)\left(p_i+s\right)}\right]^{1/(k-1)} \tag{12}$$

with $s = \sigma_c/(k-1)$. For $p_i \geqslant p_{cr}$, u_{ip} is given as:

$$u_{ip} = R\left[(1+\nu)/E\right]\left(p-p_i\right) \tag{13}$$

Suppose the permissible inward displacement is 1% of the tunnel radius. Thus the response model can be defined as:

$$g = 0.01 - u_{ip}/R \tag{14}$$

Again, five parameters (n=5) are modeled as random variables, as also shown in Table 5, that include the Young's modulus E, the cohesion h, the friction angle ϕ, the Poisson's ratio ν, and the hydrostatic stress p. A C-vine is now used with the five variables shown as

Table 5: Marginals of random variables of the tunnel excavation example

Variable	Distribution	Mean	STD
$E\ [MPa]$	Lognormal	373	48
$h\ [MPa]$	Lognormal	0.23	0.023
$\phi\ [^\circ]$	Lognormal	22.85	1.31
ν	Beta [0.2, 0.4]	0.3	0.05
$p\ [MPa]$	Beta [1.5, 3]	2	0.3

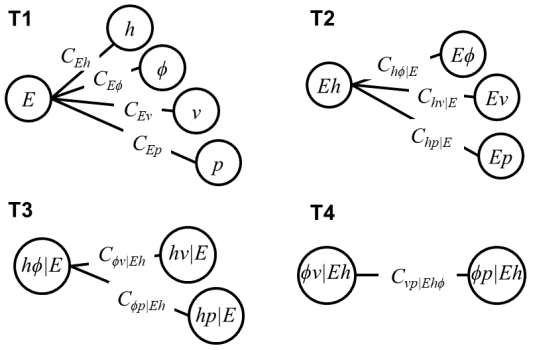

Figure 6: Vines for the tunnel excavation example

Figure 6. Various pair-copulas are assigned to each edge, such as C_{Eh}=$C_{E\phi}$=Clayton (θ=1.2), C_{Ep}=Clayton (θ=0.6), $C_{E\nu}$=Frank rotated by 90° (θ=1.5), $C_{h\phi|E}$=Frank rotated by 90° (θ=2.0) and $C_{h\nu|E}$=$C_{hp|E}$=$C_{\phi\nu|Eh}$=$C_{\phi p|Eh}$=$C_{\nu p|Eh\phi}$=Gaussian (ρ=0). Similar to the previous example, the vine copula configuration has been estimated by the sequential method in Table 2 based on 500 random samples generated from the above vine copulas.

The first four moments of the response model have been estimated by the aforementioned methods, i.e., LHS, QMC, SGH3, HPEM, and QPEM. Table 6 and Figure 7 show the estimated first four moments and their relative errors using each method, respectively. Like the previous example, the variance reduction techniques have the same sample size as the QPEM, and the SGH3's sample size is larger than the QPEM's one. The QPEM results are considerably superior in relation to all methods, particularly for skewness and kurtosis estimation. The copula-based QPEM is thus most competitive in estimating the first four moments for this case with complex dependencies between variables. By accurately estimating the first four output moments, the QPEM can also be advantageous for any reliability analysis method that relies on output moments.

Table 6: Moment estimations for the tunnel excavation example

Method	Sample size	Mean	STD	Skewness	Kurtosis
MC	10^6	0.0059	0.0009	-1.0389	4.8973
LHS	51	0.0059	0.0009	-1.6271	9.3274
QMC	51	0.0060	0.0008	-0.6905	3.1146
SGH3	61	0.0059	0.0009	-0.8611	3.3880
HPEM	11	0.0059	0.0009	-0.8056	2.8343
QPEM	51	0.0059	0.0009	-1.0223	4.6503

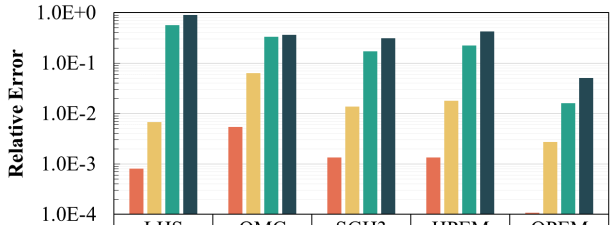

	LHS	QMC	SGH3	HPEM	QPEM
Mean	0.0008	0.0054	0.0013	0.0014	0.0001
STD	0.0068	0.0632	0.0136	0.0179	0.0027
Skewness	0.5661	0.3354	0.1711	0.2246	0.0161
Kurtosis	0.9046	0.3640	0.3082	0.4213	0.0504

Figure 7: Relative errors for tunnel excavation example

6. CONCLUSIONS

The QPEM has been recently proposed aiming to estimate accurately and efficiently, with $2n^2+1$ sample (sigma) points, probabilistic output moments of nonlinear models. The QPEM offers advantages over other PEMs in the literature in that analytical expressions for all sigma point characteristics are provided, without any need for an optimization process, and is able to completely represent up to fifth-order input moments in the Gaussian space, including the cross moments. In addition, higher-order input moment information can be uniquely incorporated by adapting the scaling parameters without any additional computational cost. As presented in this work, the QPEM can also efficiently work with general copula structures, and particularly vine copulas representing complex non-Gaussian dependencies. Two common geotechnical engineering problems presented in this work also showcased the validity, accuracy, and computational efficiency of the copula-based QPEM, for cases with non-Gaussian distributions and complex dependence structures. In both examples, the first four output moments computed by the QPEM have been compared to numerous well-known sampling methods, showcasing superior characteristics. Future work can further extend the QPEM in estimating complete output distributions, and the authors are already working toward that direction.

7. REFERENCES

Aas, K., Czado, C., Frigessi, A., and Bakken, H. (2009). "Pair-copula constructions of multiple dependence." *Insurance: Mathematics and Economics*, 44(2), 182–198.

Bedford, T. and Cooke, R. M. (2002). "Vines–a new graphical model for dependent random variables." *The Annals of Statistics*, 30(4), 1031–1068.

Cormen, T. H., Leiserson, C. E., Rivest, R. L., and Stein, C. (2022). *Introduction to algorithms*. MIT press.

Dißmann, J., Brechmann, E. C., Czado, C., and Kurowicka, D. (2013). "Selecting and estimating regular vine copulae and application to financial returns." *Computational Statistics & Data Analysis*, 59, 52–69.

Haff, I. H. (2013). "Parameter estimation for pair-copula constructions." *Bernoulli*, 19(2), 462–491.

Hoek, E. (2007). "Practical rock engineering." *Rocscience, https://www. rocscience. com/assets/resources/learning/hoek/Practical-Rock-Engineering-Full-Text.pdf*.

Hong, H. (1998). "An efficient point estimate method for probabilistic analysis." *Reliability Engineering & System Safety*, 59(3), 261–267.

Joe, H. (1997). *Multivariate models and multivariate dependence concepts*. CRC press.

Ko, M. and Papakonstantinou, K. G. (2023). "Quadratic Point Estimate Method for probabilistic moments computation." *Probabilistic Engineering Mechanics* [under review].

Li, H.-Z. and Low, B. K. (2010). "Reliability analysis of circular tunnel under hydrostatic stress field." *Computers and Geotechnics*, 37(1-2), 50–58.

Nelsen, R. B. (2007). *An introduction to copulas*. Springer.

Rosenblueth, E. (1975). "Point estimates for probability moments." *Proceedings of the National Academy of Sciences*, 72(10), 3812–3814.